MASTER

EMI reduction in an interleaved buck converter through spread spectrum frequency modulation

Stok, Emmanuel P.

Award date:
2023

Master Automotive Technology

EMI Reduction in an Interleaved Buck Converter through Spread Spectrum Frequency Modulation

MSC THESIS

Full Name	Student ID	Study
E.P.Stok	1284010	Automotive Technology

Assessment committee

Chair:	Prof.dr. G.Papafotiou
Member 1:	Dr.ir. H.Huisman
Member 2:	Dr. R.Serra
Member 3:	Dr.ir. M.R.U.Salazar
Advisory member 1:	Y.Kösesoy MSc.
Advisory member 2:	M.Otten MSc.

Graduation

Program:	Automotive Technology
Section:	Electromechanics and Power Electronics
Supervisor:	Dr.ir. H.Huisman
Date of defense:	February 15, 2023
Study load (ECTS):	45
External supervisor(s):	M.Otten

The research of this thesis has been carried out in collaboration with Lightyear.
This thesis is public and open access.

This thesis has been realized in accordance with the regulations as stated in the TU/e Code of Scientific Conduct.

EMI Reduction in an Interleaved Buck Converter through Spread Spectrum Frequency Modulation

Emmanuel Stok, *Master Student AT, TU/e, e.p.stok@student.tue.nl*

***Abstract*—EMI is a present challenge in switched mode power conversion with increasing switching frequencies, necessitating the use of EMI filters. Spread spectrum frequency modulation techniques have been applied in high frequency DC/DC power converters to reduce conducted EMI. The application of spread spectrum frequency mosulation to a 2-phase interleaved buck converter is validated through simulation and experimental testing. Using simulations, several new modulation biasing techniques are developed to further reduce EMI levels in converters equipped with hardware filters. In the lab, the new modulation techniques show and additional 1.3 dBµV reduction past the 14.2 dBµV reduction of conventional spread spectrum frequency modulation. There is an peak efficiency penalty of 0.059% in the lab, but no clear penalty at higher power levels. A large output voltage ripple is also observed.**

***Index Terms*—Interleaving, frequency modulation, EMI, buck converter, spread spectrum.**

I. INTRODUCTION

SWITCHED mode power converters are the basis for high efficiency electrical power conversion. For solar electric vehicles this is especially important, such that they can make the most of the limited solar energy they can capture [1]. Besides maximising the efficiency of the conversion action directly, the ultimate goal is maximum efficiency of the vehicle as a whole. The size and weight of the converters impact the power usage and aerodynamic performance of the vehicle.

Much work is already done in making DC/DC converters more power dense, often by increasing switching frequency and thus reducing size requirements for passive components [2]. But increased switching frequencies push the switching harmonics higher in the frequency spectrum with typically more stringent conducted electromagnetic compatibility (EMC) limits [3]. In this case, more filtering may be required to meet any applicable EMC standards. The filters must be relatively large to dampen the harmonic peaks of the switching frequency [4] at these relatively low frequencies.

Spread spectrum frequency modulation (SSFM) is a modulation strategy which can reduce the switching harmonic EMI peaks generated by the converter and is well suited for converters with high switching frequencies [4]–[14]. Originating in the communications sector [15], SSFM purposefully spreads a signal over a larger frequency band. In power converters, this is often done by modulation with a periodic signal, known as periodic SSFM [4], [6], [11], [12].

However, only [6] explores the application of SSFM to an interleaved converter. Also, there is a lack of comprehensive information regarding the effect of the modulation on efficiency.

This paper will evaluate different variations of Periodic SSFM for application in a 2-phase interleaved buck converter utilizing GaN HEMTs (shown in Fig. 1), with the goal of reducing conducted EMI. Through simulation the periodic SSFM strategy is validated for this interleaved buck and the best modulation parameters are found. A new biased SSFM strategy is also presented for converters that already include hardware EMI filters. Finally, these modulations are then applied on a hardware prototype where conducted EMI and efficiency are measured.

II. PERIODIC SPREAD SPECTRUM FREQUENCY MODULATION

A. Overview

The fundamental switching cycle of a switched mode power converter is responsible for a narrow and intense peak in the frequency spectrum, located at the switching frequency. An example is shown by the blue trace in Fig. 2. Due to the frequency composition of the square wave, this peak is followed by numerous subsequent peaks located at the harmonics of the switching frequency (not shown). By modulating the frequency of this switching cycle with SSFM, these narrow peaks devolve into a broader spectrum with a lesser peak magnitude, as shown with the first harmonic in Fig. 2.

Some parameters are introduced when discussing SSFM:

- f_c, The central switching frequency of the converter
- Δf_c, The amplitude of the modulation
- f_m, The frequency of the modulation pattern

The general effect of these parameters in the frequency spectrum is shown in Fig. 2. The Δf_c is responsible for the width of the spreading, while f_m changes the distance between the multiple spread spectrum peaks.

B. Analytical Determination of the effect of SSFM

The width of the total spreading can be estimated by Carson's Bandwidth Rule (CBR) [5],

$$\mathrm{CBR} = 2(\Delta f_c + f_m). \tag{1}$$

The resulting peak values of the SSFM are more complicated to estimate. A first estimate would be to calculate the new peak value assuming an even and flat-topped repartition of the harmonic peak signal energy into a broadband spread spectrum signal as shown in Fig. 3.

According to Parseval's Theorem, the energy of the signal can be calculated via integration in frequency domain the same

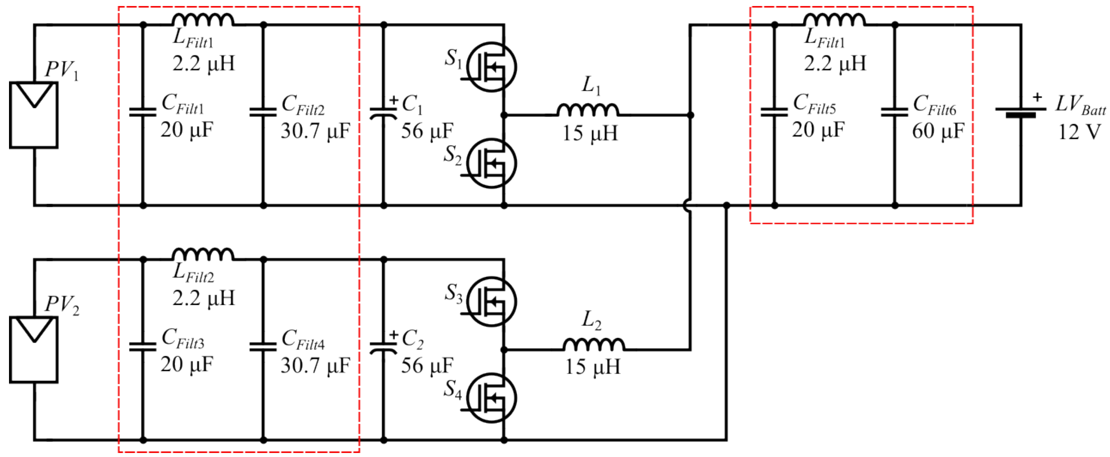

Fig. 1. Circuit schematic of the interleaved buck converter with input and output filters marked in red

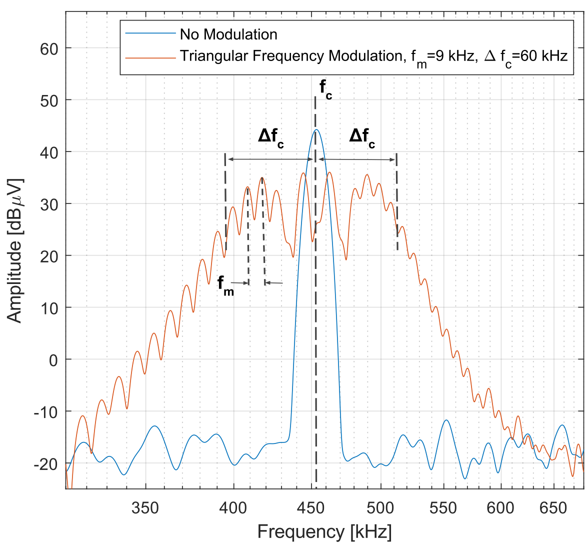

Fig. 2. The effect of basic spread spectrum modulation parameters on the average frequency spectrum measurement of the input of a buck converter, as simulated with SPICE

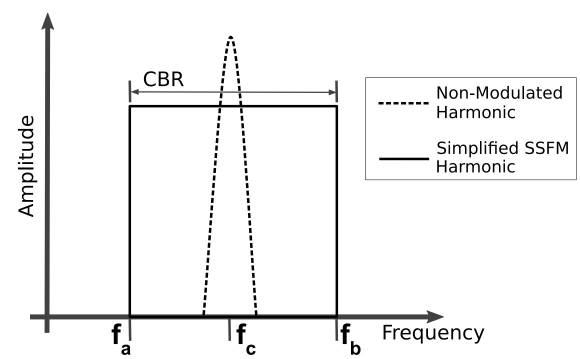

Fig. 3. A simplified representation of the effect of SSFM

as in time domain. As such, the power integration of two signals in the frequency domain can be directly compared as expressed in 2

$$\int_{f_a}^{f_b} |X_{\text{mod}}(2\pi f)|^2 \, \mathrm{d}f = \int_{f_a}^{f_b} |X_{\text{NOmod}}(2\pi f)|^2 \, \mathrm{d}f, \quad (2)$$

where X_{mod} and X_{NOmod} are the Fourier transforms of the original time domain voltage signals, and f_a and f_b are set by the CBR around the harmonic frequency of interest. In this case for the first harmonic,

$$f_a = f_c - \Delta f_c - f_m, \quad (3)$$

and,

$$f_b = f_a + \text{CBR} = f_c + \Delta f_c + f_m. \quad (4)$$

As the resulting SSFM frequency spectrum is assumed to be rectangular, 2 can be simplified to 5

$$(\text{CBR})(\text{SSFM}_{\text{peak}}) = \int_{f_a}^{f_b} |X_{\text{NOmod}}(2\pi f)|^2 \, \mathrm{d}f, \quad (5)$$

where the $\text{SSFM}_{\text{peak}}$ is the height of the simplified SSFM harmonic.

As a comparison this estimation is applied to the values that are exhibited in Fig. 2. The resulting estimated peak value for the SSFM is 32.38 dBµV, a reduction from the non-modulated peak of 11.86 dBµV. The peak value of the SSFM modulated signal as simulated in Fig. 2 is 35.61 dBµV, a reduction of 8.63 dBµV.

The reason for the discrepancy is clear from Fig. 2; the spread spectrum is not flat topped but rather a collection of lesser peaks. Each empty space between these spread spectrum peaks means the reduction is less effective. Therefore, this indicates that greatest reduction in peak values can be found with the lowest f_m and the highest Δf_c, as this results in a 'flatter' and wider spectrum.

Indeed, this is the conclusion reached by previous works on the subject [4]–[6], [11], [12], [16].

C. Implementation Limitations

The chief limit imposed on SSFM parameters is the resolution bandwidth (RBW) used in the spectrum analyzer which

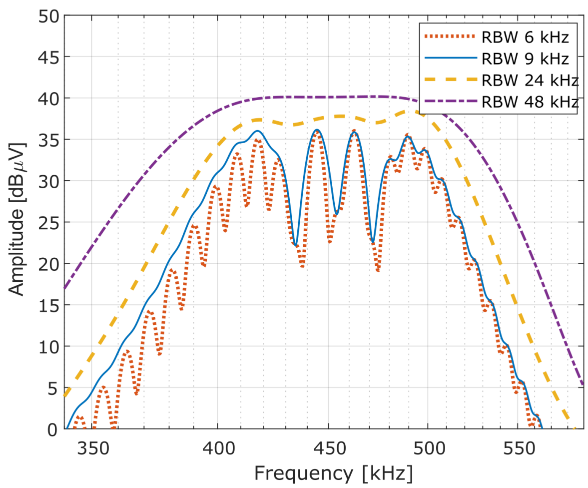

Fig. 4. The effect of RBW on average conducted EMI measurement from SPICE simulation of converter operating with $f_c = 455$ kHz, $f_m = 9$ kHz, $\Delta f_c = 60$ kHz

measures the EMI. The RBW is the width of a band-pass filter applied to the incoming signal in a spectrum analyzer. During measurement, the center frequency of this filter is swept over the measurement frequency range. The power of the signal coming through the filter is recorded for each frequency point, which generates the frequency spectrum. A wider RBW decreases measurement sweep time, however it results in a lower 'resolution' on the resulting spectrum.

If this resolution is too low, the effects of the SSFM are counteracted. Fig. 4 shows this effect as observed in a SPICE simulation of SSFM implementation. For this reason it is recommended in literature that $f_m \geq RBW$ [4], [5], [11].

To ensure this is the case the f_m must be chosen accordingly as the RBW is determined by the EMC standard. In the case of the conducted emissions measurements at the switching frequency of 455 kHz (and up to 6.2 MHz) the RBW specified by CISPR-25 is 9 kHz [3]. CISPR-25 is used in this case as a relevant automotive standard.

The other easily manipulated parameter, Δf_c, does not have such a hard limit but is limited nonetheless due to the eventual overlap of the spread spectrums in higher harmonics.

As the harmonic number increases, the center frequency of that harmonic increases with $f_h = hf_c$. In conjunction, the bandwidth of each successive harmonic increases as well [5]:

$$B_h = 2(h\Delta f_c + f_m) \tag{6}$$

with h the harmonic number.

The overlap starts to occur when:

$$f_h + \frac{B_h}{2} = f_{h+1} - \frac{B_{h+1}}{2} \tag{7}$$

which can be solved for h and simplified when presuming that $f_c \gg f_m$:

$$h_{\text{overlap}} \approx \frac{2-\delta}{2\delta} \tag{8}$$

where $\delta = \frac{\Delta f_c}{f_c}$.

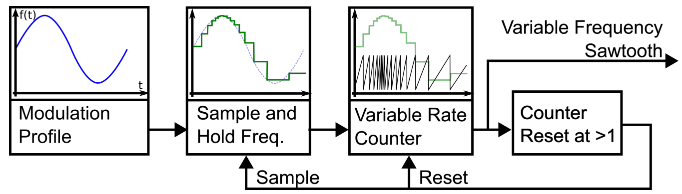

Fig. 5. Block Diagram of variable frequency sawtooth generation for use in variable frequency PWM generation

When overlap starts to occur, the peak reduction is less effective. Δf_c should be tuned to see the best reductions in the regions where they are required to meet EMI standards. Another limit on Δf_c is the sizing of passives. These must be sized for the lowest switching frequency in the modulation.

III. SSFM In Simulation

This section will examine the specifics of implementing SSFM on the interleaved buck converter and the effects of different modulation profiles. A new modulation profile to fit the case of a converter with hardware filters is presented as well. SPICE simulations are used to evaluate the difference in EMI spectra of the variations discussed. The SPICE data is exported and processed in MATLAB to emulate the effect of the RBW in a spectrum analyzer.

A. Implemention of the Modulation in Simulation

One traditional scheme for creating a PWM waveform is to compare a duty-cycle input signal with a sawtooth waveform. The output of this greater-or-less-than comparison is a PWM waveform with a duty cycle equivalent to the input, and the frequency of the sawtooth wave. This sawtooth may be modulated with the desired SSFM parameters. This is accomplished with a system which is described by the diagram in Fig. 5.

Starting from the output, the variable sawtooth is generated by a counter that resets when it hits the upper threshold. This reset triggers a sampling of the modulated frequency reference signal, which sets the slope for the next counter cycle.

The question of appropriately phase shifting the SSFM switching across the phases of an interleaved converter is investigated by [6]. The conclusion of [6] for maximum EMI reduction when applied to two phases is to dynamically delay the second phase by half of each switching period. This variable delay switching frequency modulation (VDFM) has the downside of an increased low frequency (sub-harmonic) output ripple, but the best EMI peak reduction at switching frequency and above.

B. Modulation Profiles

Three main modulation profiles are investigated by previous works: sinusoidal, triangular, and exponential [5], [11], [12], [16]. These 3 modulation profiles are summarised in Fig. 6. While each of these works claims that a triangular modulation offers more reduction than a sinusoidal modulation, [16] claims that the exponential modulation is the best while the

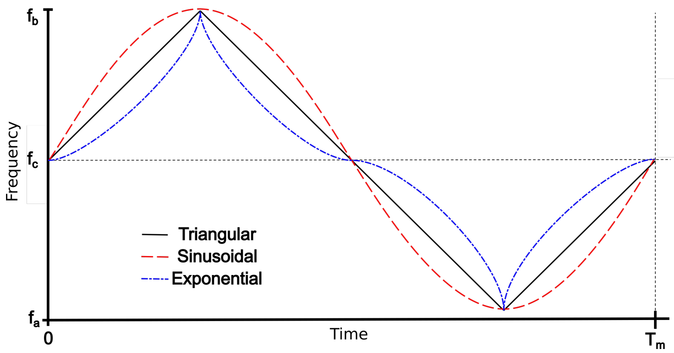

Fig. 6. Modulation profiles presented by previous works

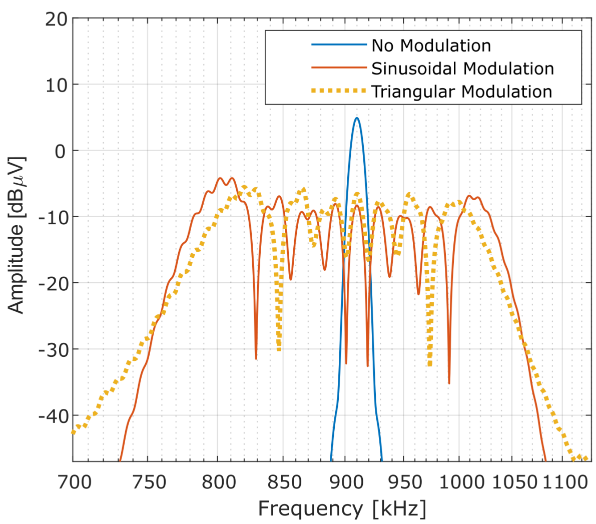

Fig. 7. Effect of modulation profiles on average conducted EMI from SPICE simulation, second harmonic. $f_m = 9$ kHz, $\Delta f_c = 60$ kHz for all modulations.

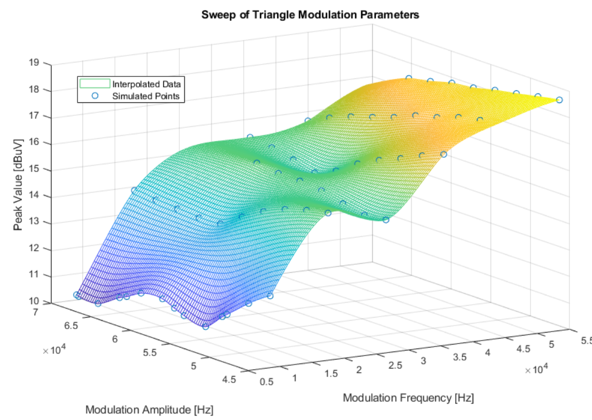

Fig. 8. A SPICE simulation sweep of f_m and Δf_c, and their effect on peak average conducted EMI values of the first harmonic for triangular SSFM, using an RBW of 9 kHz

others find the opposite. The key differences between these works is the much higher frequencies used in [16] as well as the application in clocked digital circuits rather than PWM signals in power converters.

Only sinusoidal and triangular modulation are simulated here as the application here is more in line with the frequencies and context of [5], [11], [12]. The results are shown in Fig. 7.

In Fig. 7 the sinusoidal modulated spectrum has higher peaks near the outer frequencies, but lower peaks in the center. This is due to the distribution over the frequency range of the sinusoidal modulation, where more switching happens at the frequencies near the edges of the modulation band. The triangular modulation on the other hand has a comparatively even top and thus a lower maximum peak. This effect of the modulation distribution will be exploited later.

C. Modulation Parameters

Using the simulations a sweep is performed of the f_m and Δf_c parameters in Fig 8. This is done using the triangular modulation profile, and confirms the general conclusions of previous works that a lower f_m and a higher Δf_c has lower peak values.

Some new observations, however, are that at lower values of f_m some local minima appear for the selection of Δf_c. These additional variations are rather small, at ≤ 1 dBµV between the local minima and adjacent local maxima, but so is the effect of Δf_c with ≤ 2 dBµV change over the swept range.

Compared to this, f_m has a greater effect in the lower values, but which tapers off when higher values for f_m are used.

D. Triangular Modulation Simulation Results

Shown in Fig. 9 is a view of the average conducted EMI spectrum from the interleaved converter as simulated in SPICE where the higher harmonics may be seen as well. For this simulation the converter is modelled including the filters as shown in 1, as these are also present on the hardware that will be tested later. The average conducted emissions are measured on the input side of the converter through a LISN also included in the model to match the later experimental testing setup.

The attenuation observed in this simulation is less than expected when compared to the previous literature [4]–[6], [11], [12], [16]. However, as will be seen later in section **??** the simulation used here also underestimates real world values by a significant margin. However, the relative effect of different modulations may still be evaluated through this simulation.

Despite this, a significant decrease in peak average conducted EMI values is observed. Crucially however, a significant slope is also observed along the top of the spread spectrum modulated harmonics. This is due to the LC filters (outlined in red in Fig. 1)) imposing a -40 dB/dec sloped attenuation on all frequencies above the cutoff frequency.

IV. SSFM for Filtered Applications

The previous literature referenced here on periodic SSFM use converters without filters for experimental verification. However, additional filtering may still be required for effects which are unmitigated by SSFM, or perhaps the required attenuation cannot be reached by SSFM alone.

The effect of additional hardware filtering can be taken advantage of in the modulation. As the hardware filters impart

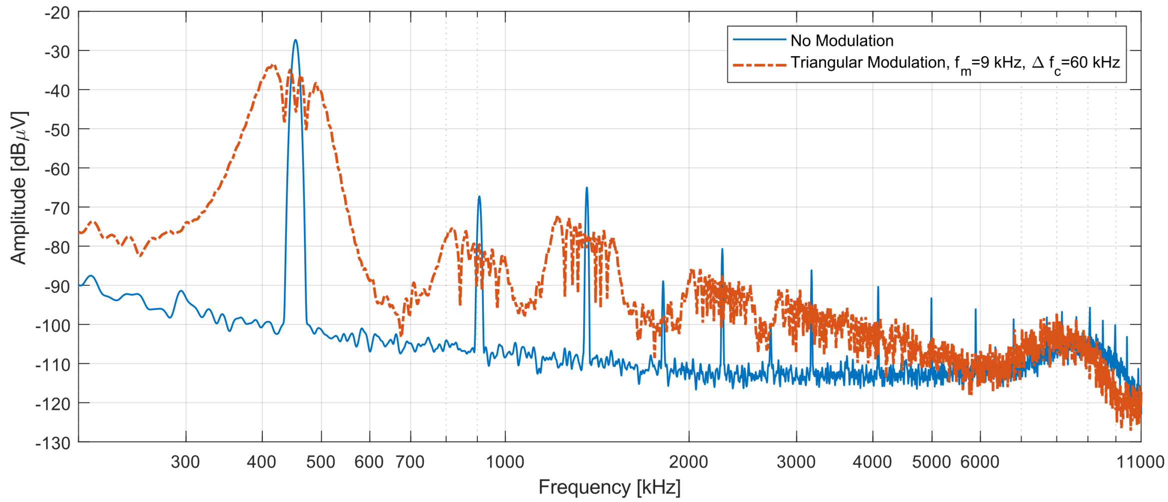

Fig. 9. Triangular SSFM average conducted emissions in SPICE simulation, input of interleaved buck converter with hardware LC filters.

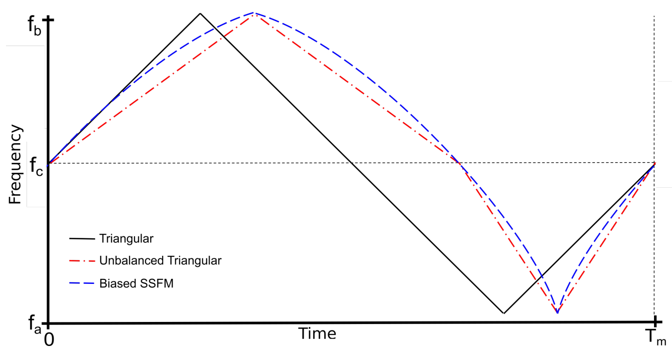

Fig. 10. Two new modulation profiles to shift the switching frequency balance towards the higher frequencies

more attenuation on higher frequencies, the modulation can be biased to shift more energy into the region above center frequency.

A. Unbalanced Triangular Modulation

With a simple modification to the triangular modulation, the weight of the spread spectrum can be shifted. The unbalanced triangular profile in Fig. 10 is presented as a simple approach to obtain further peak reduction. Here, the amount of time spent switching above f_c in every modulation period is increased, thus putting more energy into the high side of the spectrum.

Compared to normal triangular modulation, using the unbalanced triangular profile with 55% of time spent above the center frequency 1.36 times more reduction on the first harmonic and 1.17 times on the third harmonic is achieved in SPICE simulation. The spectrum for this is shown in Fig. 11.

Yet as seen in Fig. 11, the unbalanced triangular spectrum does not make the spread spectrum harmonic peak flat-topped. Rather, the effect can be described as breaking up the sloped spread spectrum into two separate regions such that one may be offset without really counteracting the slope of the filter.

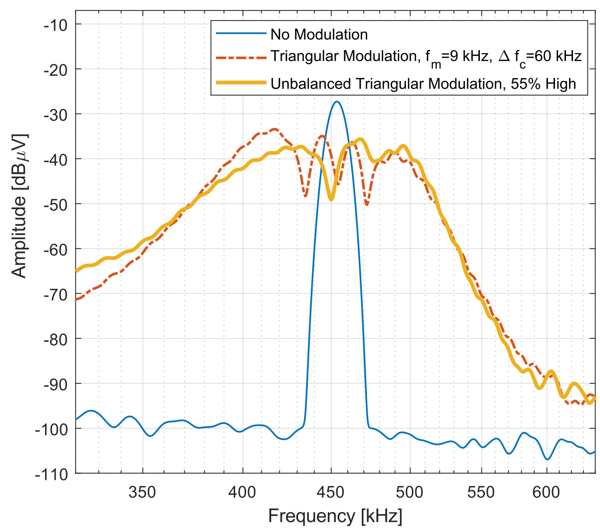

Fig. 11. Average conducted EMI of unbalanced triangular modulation and triangular modulation on input of interleaved buck converter as simulated in SPICE.

B. Biased Modulation

To better take advantage of the damping shape of the filters a biased modulation profile is developed. This modulation profile is generated by working backwards from the desired shape of the resulting EMI spectrum.

As was observed previously, the distribution of the modulating signal shapes the envelope of the resulting EMI spectrum. In other words, the envelope of the resulting EMI spectrum of these modulated signals is an imprint of the probability density function (PDF) of the modulating signal (in dB).

As the slope imparted on the spectrum by a first order LC filter is -40 dB/dec, the modulation generates a spectrum which has a +40 dB/dec slope (before filtering). Converting to the

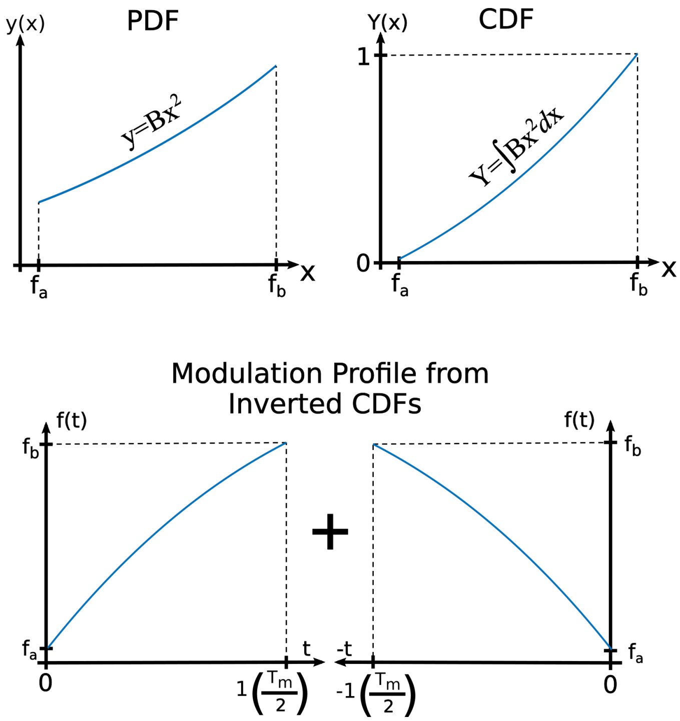

Fig. 12. Process for generating a modulation profile from a desired probability density function by inverting and scaling the CDF

linear space, the modulating signal has a PDF describable by

$$y = Bx^2. \tag{9}$$

The selection of the coefficient B is based on the range of frequencies for that particular modulation. The integral of a PDF should be equal to 1, so

$$1 = \int_{f_a}^{f_b} Bx^2 dx. \tag{10}$$

From this, the coefficient B can be solved

$$B = \frac{3}{f_b^3 - f_a^3}, \tag{11}$$

where f_{min} and f_{max} are the limits of the desired modulation range. For a modulation with center $f_c = 455$ kHz and modulation amplitude $\Delta f_c = 60$ kHz an example PDF is shown in Fig. 12.

While a PDF is not unique to a particular function, it can be used to create a modulation profile. By integrating the PDF, the cumulative distribution function (CDF) is found, shown in Fig. 12. The CDF may be inverted and the new horizontal axis scaled to create a function in time with the same PDF/CDF.

In this case, the inverted CDF is combined with its reflection across the vertical axis to create a continuous and cyclical function, then scaled to match modulation frequency f_m. The resulting function in time is the "Biased SSFM" modulation profile shown in 10.

This profile is simulated in SPICE, and the peak reduction is similar to the unbalanced triangular modulation. However, as seen in Fig. 13 the slope along the top of the peaks is once again consistent as opposed to the unbalanced triangular modulation in Fig. 11.

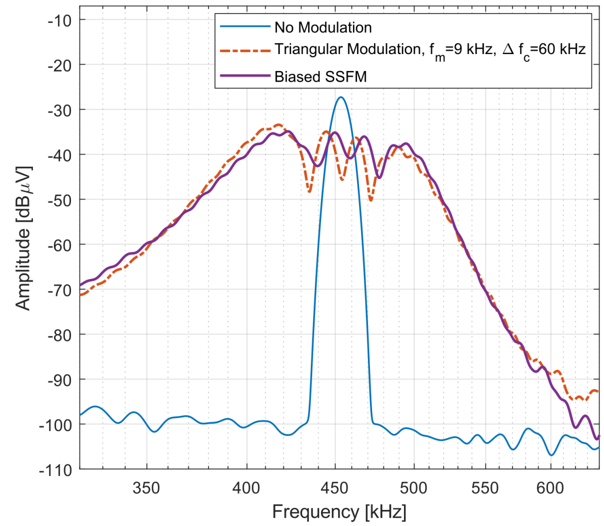

Fig. 13. Average conducted EMI of biased SSFM modulation and triangular modulation at the input of the interleaved buck converter as simulated in SPICE

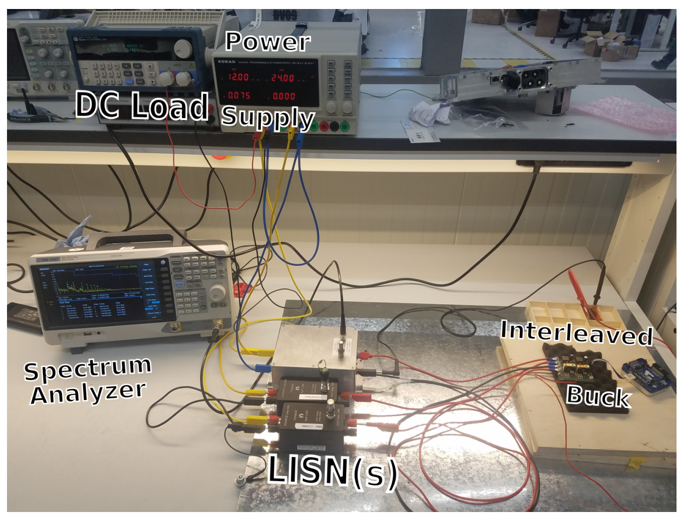

Fig. 14. EMI testing setup

V. Experimental Testing

A. EMI Testing Setup

Shown in Fig. 14 is the testing setup used for the average level conducted emissions testing on one of the inputs of the converter. This setup is as described in CISPR-25 [3], though with some differences. There is no shielded chamber, and thus the ground plane is also not bonded to the floor. The ground plane does not meet the minimum size spec, but is large enough to accommodate the device distance to edge specifications.

Some steps were taken to isolate the system from the grid connections, but due to equipment limitations some interfaces had to remain in place. While the micro-controller was powered by a battery, the main power loop still needed a bench power supply for the two 24 V inputs and an active DC load for the fixed 12 V output. Care was taken to place line impedance stabilization networks (LISNs) on each of these connections to isolate as much outside noise as possible, but as the later results will show this was not entirely successful.

The spectrum analyzer parameters are within the limits described in CISPR-25 for these measurments. The spectrum analyzer is a Siglent SSA3021X Plus. The RBW is set at 9 kHz, the video bandwidth at 30 kHz, the step size at less than 5 kHz, and a little over 319 ms measurement time at each step. Only average detector measurements are taken in this paper, but [6] shows peak detector readings to be very similarly impacted by SSFM and the same is expected here.

B. Average Conducted EMI of SSFM

Shown in Fig. 16 are the average conducted emissions of the converter operating under triangular modulation and biased modulation both for 60 kHz and 100 kHz modulation amplitudes (with no modulation case for reference). Table I shows the peak values of the first harmonic. Due to range of the SSFM applied, this peak value of the first harmonic is taken in the range of frequencies from 355 kHz to 555 kHz.

TABLE I
PEAK MEASURED AVERAGE EMI VALUES OF THE FIRST HARMONIC FOR VARIOUS SSFM MODULATIONS

Modulation	Peak Value in First Harmonic [dBμV]	Peak Reduction [dBμV]
No Modulation	56.82	-
Triangular Modulation $\Delta f_c = 60$ kHz	42.97	13.85
Triangular Modulation $\Delta f_c = 100$ kHz	42.61	14.21
Biased Modulation $\Delta f_c = 60$ kHz	43.21	13.61
Biased Modulation $\Delta f_c = 100$ kHz	41.31	15.51

As shown in Table I, the peak value reduction achieved on the first harmonic is very similar between modulation types and amplitudes. Less than 2 dBμV of difference in the peak values of the different modulations are observed. At higher harmonics, the different modulations become indistinguishable in terms of peak reduction.

However, some clear peaks are visible in Fig. 16 in some of the modulations. These are most visible in the triangular modulation with $\Delta f_c = 100$ kHz at frequencies of 648, 728, 810, and 890 kHz. These non-harmonic peaks also visible in other modulations and other frequencies. These peaks are intermittently observed in the measurements of every modulation, including in the case shown in Fig. 15 where the converter is powered off but still connected to the setup.

As these peaks are not observed when the bench supply and active load are unplugged from the grid, it is concluded that this noise does not originate from within the converter or modulations tested here.

Despite this, a closer look at the first harmonic can still confirm the expected effects of biasing the modulations. In both the 60 kHz amplitude and 100 kHz amplitude modulations (shown in Fig. 17 and Fig. 18, respectively) the biased modulation works to manipulate the shape of the spectrum.

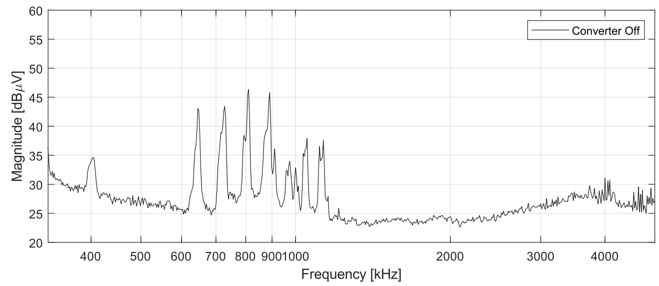

Fig. 15. Conducted EMI measurements with the buck converter off, but still connected to the setup

In the 60 kHz modulations, the spectrum envelope of the triangular modulation is inconsistently sloped to begin with. Despite shifting the spectrum as intended the biasing performs worse by 0.24 dBμV. In this case the highest peak was still at f_c, which is not significantly affected by the biasing.

With the larger amplitudes of the 100 kHz modulations however, a more consistently sloped region of the spectrum is observed. This region is better flattened by the biasing and an additional 1.3 dBμV reduction is achieved.

C. Efficiency Testing Setup

For testing the efficiency the setup is similar to the EMI testing, but without the LISNs. A PPA5500 3-channel power analyzer with internal shunts and remote voltage sensing is used to measure the voltage and current of the two input phases and single output of the converter.

The gate driving circuitry is powered on-board and so these losses are taken into account. However, the micro controller is again powered separately. Any additional power consumed in processing is therefore not included in the following results. As the constant application of a new switching frequency is required to successfully carry out the modulation, some more processing capability (or more specialized hardware such as an FPGA) is required.

It was noted during testing that depending on the code implementation and compiler settings, the power consumption of the micro controller could increase to a point which is significant at these power levels. The micro controller power consumption was not included in the efficiency results.

D. The effect of SSFM on Efficiency

Shown in Fig. 20 is a collection of efficiencies of operation with unbalanced triangular modulations which are progressively more biased towards higher frequency switching. With this converter, spending more time switching at the frequencies above 455 kHz appears to have little effect on efficiency. It should also be noted that the unbalanced triangular modulation with 62% of the switching time above 455 kHz is the closest match to the biased SSFM modulation profile. The 75% unbalanced triangular modulation is included to investigate the extremes of the useful application of this technique.

Next, Fig 21 shows two different modulations with a similar distribution of frequencies but for different modulation amplitudes. Here there is again no clear difference in efficiency.

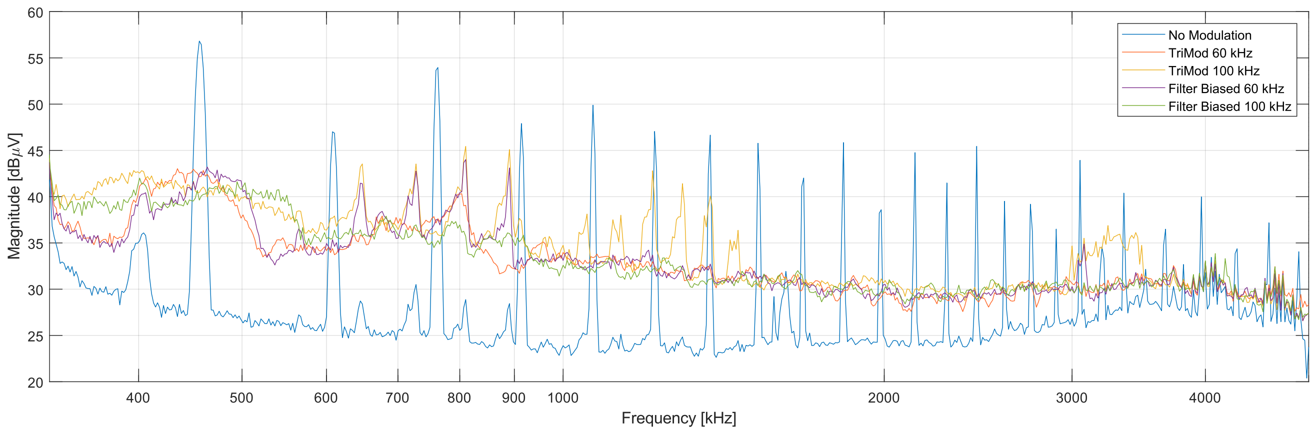

Fig. 16. Average conducted emissions measured on the converter input, from 340 kHz to 4 MHz

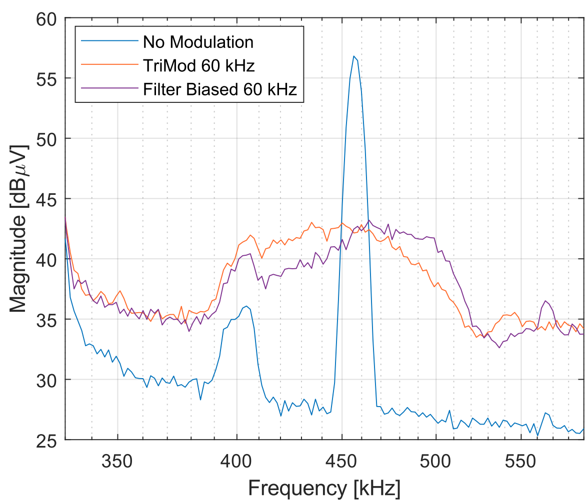

Fig. 17. Average conducted emissions around the first harmonic measured on the converter input for 60 kHz amplitude modulations

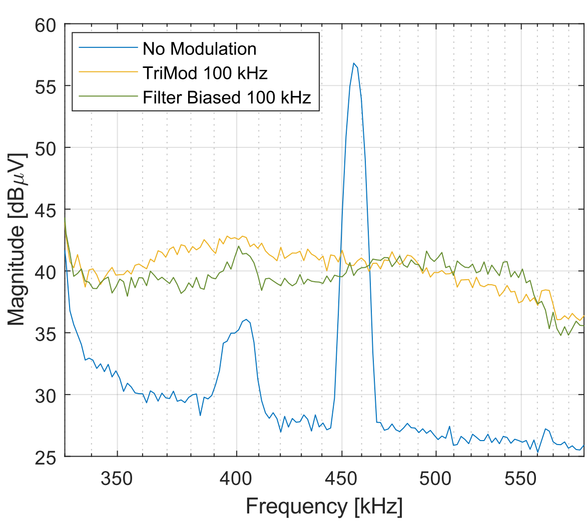

Fig. 18. Average conducted emissions around the first harmonic measured on the converter input for 100 kHz amplitude modulations

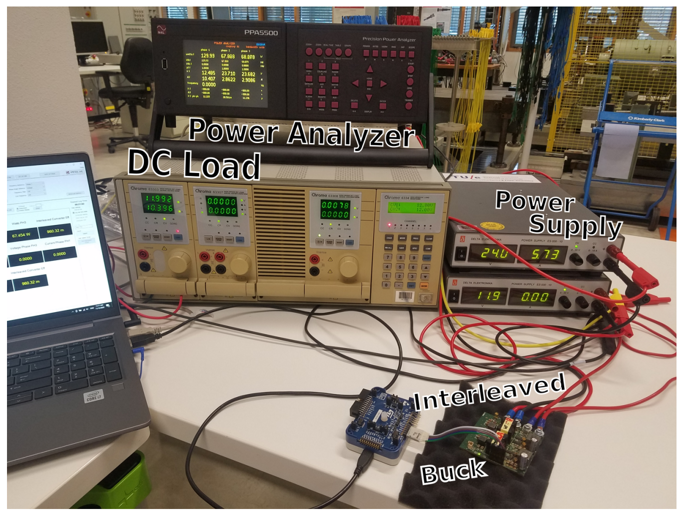

Fig. 19. Efficiency testing setup

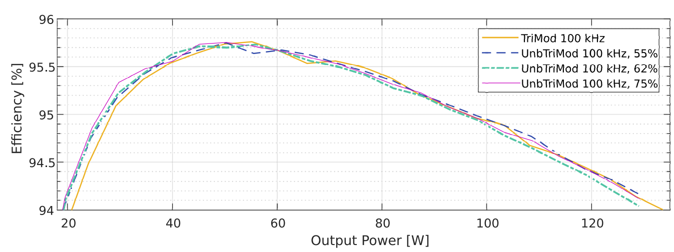

Fig. 20. Efficiency of higher frequency biased modulations

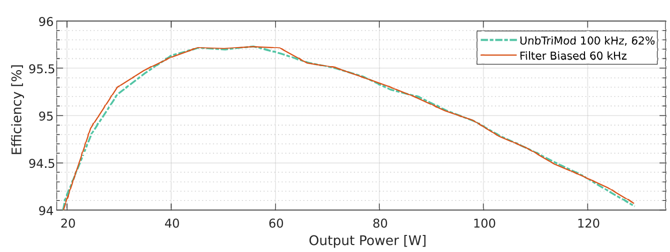

Fig. 21. Efficiency of higher amplitude modulations

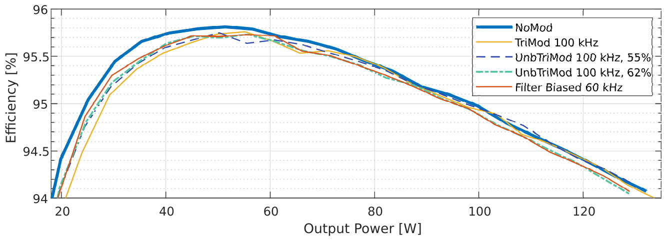

Fig. 22. Comparison of modulated efficiency to non-modulated efficiency

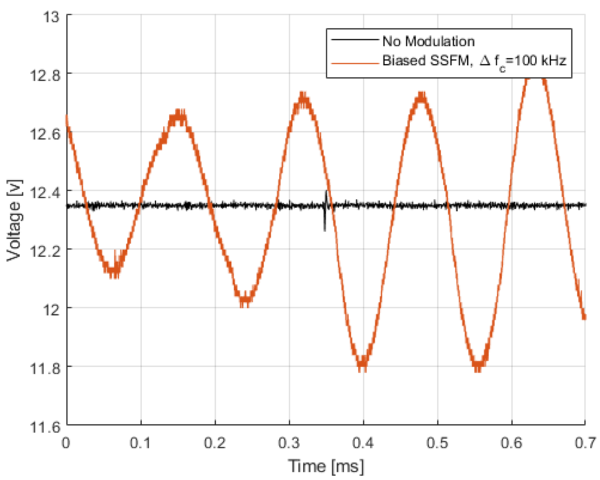

Fig. 23. Voltage ripple measured on the interleaved buck converter output

Finally, Fig. 22 shows this selection of modulations against the non-modulated case. Here there is an observable difference to the operational efficiency of the converter at lower powers, up to and including the peak efficiency point at around 51 W output power. When any SSFM profile is used, around 0.059% of efficiency is lost from the peak efficiency. This is around 29.5 mW of additional losses in this converter.

At higher power levels there is no longer a clear difference in efficiency between the modulated and non-modulated modes of operation.

E. Output Voltage Ripple

As reported in [6], an increased sub-harmonic output voltage ripple is observed when the VDFM SSFM used here is applied. However, while the ripple reported in [6] is 23.3 mV_{pp}, the ripple in the converter used here is orders of magnitude larger as shown in Fig. 23. Ranging between 0.5 V_{pp} to 1 V_{pp} the ripple is not consistent over time, but is observed regardless of the variation of the modulation used.

While the ripple is fundamentally caused by the patterns of the modulation, its magnitude is influenced by dead time, component sizing, and the load characteristics. But crucially, [17] shows that with properly selected output voltage control the ripple can be drastically limited which is the case in [6] but not here as the converter is run in open loop.

VI. Future Work

As explained in the previous section, the ripple can likely be limited by the inclusion of some output voltage control. Particularly for the sake of efficiency this should be investigated further as it is probable that this ripple is a cause for the decrease in efficiency when using the modulation.

Further, the EMI measurements taken here clearly have some faults. Some better isolated measurements would be beneficial in more closely evaluating the effect of the modulation at the second or third harmonics. Even around the first harmonic, the bump in noise present at 400 kHz obfuscates the shape of the low frequency side of the first harmonic in the modulated measurements.

Finally, the shaping of the EMI spectrum through altering the distribution of the modulating signal offers an opportunity for finer tuning of the spectrum. This could be exploited to further flatten and reduce peaks in the spectrum, although at that point the tuning would likely be converter specific. Perhaps some learning algorithm could be applied for this, although the question of adequate sensing for the feedback would remain a challenge.

VII. Conclusion

The theory of SSFM and a simplified analytical analysis is presented. The limitations of the technique as presented by previous works are explored. Some simulations of the technique are carried out to verify the applicability of the referenced literature conclusions when applied to the two phase interleaved buck converter examined in this paper.

The shortcomings of previously presented modulation schemes in regards to a converter with hardware filters are observed, and some new modulation profiles are presented to deal with these limitations.

Finally, hardware tests of these techniques reveal some trade-offs in other areas of converter performance. Some effect on efficiency is noticeable in lower power levels but are of lesser consequence in higher powers. Some increased computation requirements are present. A pronounced output voltage ripple can be observed in open loop operation, likely necessitating closed loop control for many applications. Despite these limitations, SSFM is an effective tool to reduce conducted EMI around the switching harmonics. In the application of a filtered converter the biasing of the modulation can be effective for further reduction of conducted EMI.

References

[1] C. R. Sullivan and M. J. Powers, “A high-efficiency maximum power point tracker for photovoltaic arrays in a solar-powered race vehicle,” 1993.

[2] H.-P. Park, H.-J. Choi, and J.-H. Jung, “Design and implementation of high switching frequency llc resonant converter for high power density,” in *2015 9th International Conference on Power Electronics and ECCE Asia (ICPE-ECCE Asia)*, 2015, pp. 502–507.

[3] *Vehicles, boats and internal combustion engines - Radio disturbance characteristics - Limits and methods of measurement for the protection of on-board receivers*, CISPR-25, 2016.

[4] J. Balcells, A. Santolaria, A. Orlandi, S. Member, D. González, and J. Gago, “Emi reduction in switched power converters using frequency modulation techniques,” *IEEE TRANSACTIONS ON ELECTROMAGNETIC COMPATIBILITY*, vol. 47, p. 569, 2005.

[5] A. Santolaria, J. Balcells, and D. Gonzalez, “Theoretical and experimental results of power converter frequency modulation,” 2002.
[6] J. Mon, D. González, J. Balcells, J. Gago, and P. Bogónez, *Hybrid Modulator for power converters in parallel topology*, 2012.
[7] M. M. Bech and J. K. Pedersen, “Random modulation techniques with fixed switching frequency for three-phase power converters,” p. 753, 2000.
[8] G. M. Dousoky, S. Member, M. Shoyama, S. Member, and T. Ninomiya, “Fpga-based spread-spectrum schemes for conducted-noise mitigation in dc-dc power converters: Design, implementation, and experimental investigation,” *IEEE Transactions on Industrial Electronics*, vol. 58, p. 429, 2011.
[9] H. Li, Y. Liu, J. Lü, and X. Yu, “Suppressing emi in power converters via chaotic spwm control based on spectrum analysis approach,” *IEEE TRANSACTIONS ON INDUSTRIAL ELECTRONICS*, vol. 61, 2014.
[10] K. K. Tse, R. W.-M. Ng, H. S.-H. Chung, and S. Y. R. Hui, “An evaluation of the spectral characteristics of switching converters with chaotic carrier-frequency modulation; an evaluation of the spectral characteristics of switching converters with chaotic carrier-frequency modulation,” *IEEE Transactions on Industrial Electronics*, vol. 50, 2003.
[11] D. González, J. Balcells, A. Santolaria, J.-C. L. Bunetel, J. Gago, D. Magnon, and S. Bréhaut, “Conducted emi reduction in power converters by means of periodic switching frequency modulation,” *IEEE TRANSACTIONS ON POWER ELECTRONICS*, vol. 22, 2007.
[12] A. Santolaria, J. Balcells, D. Gonzalez, and J. Gago, “Evaluation of switching frequency modulation in em1 emissions reduction applied to power converters,” 2003.
[13] S. U. Hasan and G. E. Town, “An aperiodic modulation method to mitigate electromagnetic interference in impedance source dc-dc converters,” *IEEE Transactions on Power Electronics*, vol. 33, pp. 7601–7608, 9 2018.
[14] S. Johnson and R. Zane, “Custom spectral shaping for emi reduction in high-frequency inverters and ballasts,” *IEEE TRANSACTIONS ON POWER ELECTRONICS*, vol. 20, p. 1499, 2005.
[15] R. C. Dixon, *Spread Spectrum Systems*. J. Wiley, 1984.
[16] K. B. Hardin, J. T. Fessler, and D. R. Bush, “Spread spectrum clock generation for the reduction of radiated emissions,” 1994.
[17] D. González, J. T. Bialasiewicz, J. Balcells, and J. Gago, “Wavelet-based performance evaluation of power converters operating with modulated switching frequency,” *IEEE Transactions on Industrial Electronics*, vol. 55, pp. 3167–3176, 2008.